# Control of Surface and $\zeta$ Potentials on Nanoporous TiO$_2$ Films by Potential-Determining and Specifically Adsorbed Ions

Bryce P. Nelson,[†] Roberto Candal,[‡,§] Robert M. Corn,[†] and Marc A. Anderson*,[‡]

*Water Chemistry Program, University of Wisconsin–Madison, 660 North Park Street, Madison, Wisconsin, 53706, and Department of Chemistry, University of Wisconsin–Madison, 1101 University Avenue, Madison, Wisconsin 53706*

The effect of a specifically adsorbed ion, phosphate, on the electrochemical response and adsorption properties of nanocrystalline TiO$_2$ is examined. Phosphate is known to affect the $\zeta$ potential, as measured by electrophoretic mobility, by changing the charge of the oxide surface. The adsorption of a cationic probe molecule, thionine, onto TiO$_2$ was monitored with an in-situ cell using UV–vis spectroscopy. The adsorption of the cationic dye molecule was found to be governed by changes in the $\zeta$ potential, whether the $\zeta$ potential was modified by pH or by changes in phosphate concentration. Onset potential measurements were used to estimate the flat-band potential of a Ti/TiO$_2$ electrode. The flat-band potential results for the electrode showed a nearly Nernstian response to changes in the pH for a broad pH range. The addition of phosphate had no effect on the onset potential or on the shape of the photocurrent/potential curve. Flat-band potentials determined by Mott–Schottky analysis in the absence of phosphate were Nernstian only for pH 3–7, matching the pH dependence of the electrophoretic mobility results. With the addition of phosphate, impedance spectroscopy results showed additional space charge capacitance, peaking at potentials 150 mV positive of the flat-band potential. UV irradiation also resulted in an additional space charge capacitance. For both cases, the additional space charge capacitance was accompanied by a decrease in the resistance of the electrode, as shown in Nyquist plots. The change in film conductivity is believed to affect the space charge layer capacitance. Similarly, a decrease in film resistance was also seen with lower pH values. Currently, this change in TiO$_2$ film conductivity with surface acidity is being investigated in our laboratory for application in fuel cell electrolytes.

## Introduction

Adsorption of ions onto colloids and surfaces has been well studied in a variety of systems, yet a clear understanding of the role of specifically adsorbed ions at the oxide/water interface remains elusive. Of particular interest is TiO$_2$, which has become an important material for use in solar cells,[1,2] energy storage devices,[3] and electrochromic devices[4] and for use in the degradation of organic contaminants in both air and water.[5–11] The viability of these technologies has been enhanced by reports indicating that adsorption of various organic molecules onto the TiO$_2$ surface can sensitize these materials to the visible part of the spectrum.[12–14] Recently, our laboratory investigated TiO$_2$ as a possible material for use in fuel cells.[15,16]

All of these applications depend on a proper understanding of the surface chemistry at the oxide/water interface. Using electrophoretic mobility and surface titrations, past studies [10,17–21] characterized electrolytes as belonging to one of three different categories. Protons and hydroxide ions are called potential-determining ions for oxides such as TiO$_2$ in aqueous solution. These ions control the surface potential of TiO$_2$ according to the Nernst equation. Potential-determining ions also affect the $\zeta$ potential (the potential at the plane of shear, a distance slightly removed from the diffuse part of the double layer) such that the point of zero $\zeta$ potential (pzzp) is moved in an electrophoretic mobility experiment. Indifferent electrolytes, such as potassium and nitrate

* Corresponding author. E-mail: (nanopor@facstaff.wisc.edu. Fax: (608) 262-0454. Phone: (608) 262-2674.
† Department of Chemistry.
‡ Water Chemistry Program.
§ Present address: INQUIMAE, Universidad de Buenos Aires, Ciudad Universitaria, Pabellón 2, Buenos Aires CP 1428, Argentina.

(1) Bach, U.; Lupo, D.; Comte, P.; Moser, J. E.; Weissortel, F.; Salbeck, J.; Spreitzer, H.; Gratzel, M. *Nature* **1998**, *395*, 583–585.
(2) O'Regan, B.; Grätzel, M. *Nature* **1991**, *353*, 737.
(3) Papageorgiou, N.; Grätzel, M. *Abs. Pap.—Am. Chem. Soc.* **1998**, *215*, 232.
(4) Bechinger, C.; Ferrere, S.; Zaban, A.; Sprague, J.; Gregg, B. A. *Nature* **1996**, *383*, 608.
(5) Ollis, D. E., Al-Ekabi, H., Eds. *Photocatalytic Purification of Water and Air*; Wiley-Interscience: Amsterdam, 1993.
(6) Pichat, P.; Herrmann, J. M. *Photocatalysis. Fundamentals and Applications*; Wiley: New York, 1989.
(7) Serpone, N.; Pelizzetti, E. *Photocatalysis Fundamentals and Applications*; Elsevier: Amsterdam, 1993.
(8) Bahnemann, D.; Cunningham, J.; Fox, M. A.; Pelizzetti, E.; Pichat, P.; Serpone, N. *Aquatic and Surface Photochemistry*; Lewis: Boca Raton, FL, 1994.
(9) Pichat, P., Ertl, G., Knözinger, H., Weitkamp, J., Eds. *Handbook of Heterogeneous Photocatalysis*; VCH: Weinheim, Germany, 1997; Vol. 4, p 2111.
(10) Furlong, D. N.; Wells, D.; Sasse, W. H. F. *J. Phys. Chem.* **1985**, *89*, 626–635.
(11) Mills, A.; Hunte, S. L. *J. Photochem. Photobiol., A* **1997**, *108*, 1.

(12) Yan, S. G.; Hupp, J. T. *J. Phys. Chem.* **1996**, *100*, 6867–6870.
(13) Kay, A.; Humphery-Baker, R.; Gratzel, M. *J. Phys. Chem.* **1994**, *98*, 952–959.
(14) Vinodgopal, K.; Hua, X.; Dahlgren, R. L.; Lappin, A. G.; Patterson, L. K.; Kamat, P. V. *J. Phys. Chem.* **1995**, *99*, 10883.
(15) Vichi, F. M.; Tejedor-Tejedor, M. I.; Anderson, M. A. *Chem. Mater.,* in press.
(16) Vichi, F. M.; Colomer, M. T.; Anderson, M. A. *Electrochem. Solid State Lett.* **1999**, *2*, 313–316.
(17) Hunter, R. J. *Zeta Potential in Colloid Science*; Academic Press: New York, 1981.
(18) Akratopulu, K. C.; Kordulis, C.; Lycourghiotis, A. *J. Chem. Soc., Faraday Trans.* **1990**, *86*, 3437–3440.
(19) Jaffrezic-Renault, N.; Pichat, P. *J. Phys. Chem.* **1986**, *90*, 2733–2738.
(20) Anderson, M. A.; Malotky, D. T. *J. Colloid Interface Sci.* **1979**, *72*, 413–427.
(21) Anderson, M. A.; Rubin, A. J. *Adsorption of Inorganics at Solid-Liquid Interfaces*; Ann Arbor Science Publishers: Ann Arbor, MI, 1981.

ions, can affect the $\zeta$ potential through charge screening but cannot change the pzzp. A third type of ions, specifically adsorbed ions, also called "potential-determining ions of the second kind", have a more ambiguous character. Despite the fact that the adsorption of these ions dramatically affects the potential of the diffuse part of the double layer, it does not affect the surface potential. However, these ions do dramatically affect the $\zeta$ potential and will move the pzzp similarly to potential-determining ions.[20] Chemical models consider the adsorption of specifically adsorbed ions as occurring in a layer different from that in which potential-determining adsorb.[21] On the other hand, CIR−FTIR spectroscopy has been used to demonstrate that phosphate chemically binds to TiO$_2$,[22] and it is agreed that specific adsorption occurs at the inner part of the double layer.[17] A more thorough understanding of this topic is necessary to precisely control these oxide surfaces.

In our laboratory, coated nanocrystalline TiO$_2$ electrodes have been used for some time for the photocatalytic degradation of organic contaminants in air and water. The colloidal nature of porous nanocrystalline thin-film oxide electrodes coupled with their semiconductor properties makes these surfaces complicated. While the exact nature of the interface is still uncertain,[23] it is believed that when the electrode is placed in solution, the electrolyte penetrates the porous network in such a way that electrochemical and adsorption processes take place throughout the porous network.[24,25] Penetrating inorganic ions such as phosphate have been shown to adsorb strongly to the surface of TiO$_2$ and affect the utility of the coating. Vichi et al. recently reported that phosphate adsorption can increase the proton conductivity of a TiO$_2$ xerogel.[15] In the photocatalytic degradation process, these ions may either block active sites on the TiO$_2$ catalyst or compete with organic contaminants for oxidizing radicals during the photocatalysis process.[22] Abdullah et al.[26] showed that the presence of phosphate in solution reduced the rate of photocatalyzed oxidation of model organic contaminants by as much as 70%. Since aqueous-phase photoelectro-catalysis and photocatalysis in particular suffer from low photoefficiency, a clearer understanding of the TiO$_2$/water interface is necessary for these technologies to become viable.

By coating porous nanocrystalline oxide films onto metallic supports, one may control and analyze the potential at the surface of oxide systems in ways previously unavailable to colloid chemists. Nanocrystalline particles are believed to be too small to form a semiconductor depletion layer. Despite this, electrochemical biasing of oxide thin films has been shown to affect the interface; an electrochemical bias at a potential positive of the flat-band potential has been shown to improve rates of photocatalysis on nanocrystalline TiO$_2$.[27] Moreover, in TiO$_2$ systems with a titanium backcontact, Mott−Schottky behavior has been demonstrated and attributed to the oxide layer on the backcontact.[28] However, the determination of the flat-band potential, while an effective probe

of the potential at the surface, has proven difficult because of complications such as surface states and other imperfections on the oxide surface. Therefore, in this study, several techniques were used to examine fluctuations in potential at the oxide surface. One such technique, impedance analysis, was used previously to study the capacitance and flat-band potential of nanocrystalline TiO$_2$ films supported on titanium backcontacts[28,29] and on conductive glass.[24,25]

In determining the flat-band potential, it is important to recall some fundamental aspects of semiconductor electrochemistry. When an n-type semiconductor, such as TiO$_2$, is exposed to a solution, charge transfer must occur to bring the two phases to electrostatic equilibrium at the interface. Unlike a metal, where excess charge resides at the surface, charge in a semiconductor forms a "space charge layer" near the surface, since charge is not free to move about in the semiconductor. The electric field that forms the space charge layer is also known as band bending.[30] At some applied potential, these bands become flat, and the potential in the bulk of the semiconductor is equilibrated with that of the solution. Kavan et al.[31] compared the behavior of single-crystal anatase with single-crystal rutile and found the flat-band potential of anatase to have a Nernstian-type pH dependence in aqueous media. The measurement of the flat-band potential of porous semiconductor electrodes can be used to aid in understanding surface potential, especially when compared to electrophoretic mobility measurements of colloidal suspensions of the same oxide. Previous authors have shown that changes in local pH can occur during the photooxidation process when TiO$_2$ in water is exposed to UV irradiation. These changes were shown to lead to variations in band bending and changes in the flat-band potential.[32] In this paper, we demonstrate how changes in adsorbed species on the surface such as hydronium and hydroxide ions, as well as protolyzable anions such as phosphate and arsenate, can be used to control the adsorption of charged molecules, affect the space charge layer, and even affect surface conductivity.

## Experimental Section

**Materials.** Titanium backcontacts were fabricated from 3 × 3 cm squares of a 0.05 mm thick titanium foil (Goodfellow Cambridge Ltd.). All other chemicals were analytical reagents of the highest available purity. Millipore-filtered water was used for all rinsing and aqueous solutions. Details concerning the preparation of the titanium-supported TiO$_2$ photoelectrode are available elsewhere.[33] Electrodes were prepared as follows: (i) Titanium supports were cleaned in an ultrasonic acetone bath. (ii) Cleaned plates were dip-coated with one layer of *tert*-amyl alcohol-based TiO$_2$ sol[34] (particle size 5 nm) at a withdrawal speed of 1.5 cm/min. iii) Plates coated with alcohol-based sol were sintered at 450 °C for 1 h. (iv) Sintered plates were dip-coated a second time with aqueous-based TiO$_2$ sol[35] (particle size 80 nm) at the

(22) Tejedor-Tejedor, M. I.; Vicchi, F. Unpublished results, 1998.
(23) Shiga, A.; Tsujiko, A.; Ide, T.; Nakato, Y. *J. Phys. Chem. B* **1998**, *102*, 6049−6055.
(24) Wahl, A.; Augustynski, J. *J. Phys. Chem. B* **1998**, *102*, 7820−7828.
(25) Cao, F.; Oskam, G.; Searson, P. C.; Stipkala, J. M.; Heimer, T. A.; Farzad, F.; Meyer, G. J. *J. Phys. Chem.* **1995**, *99*, 11974−11980.
(26) Abdullah, M.; Low, G. K.-C.; Matthews, R. W. *J. Phys. Chem.* **1990**, *94*, 6820−6825.
(27) Kim, D. H.; Anderson, M. A. *Environ. Sci. Technol.* **1994**, *28*, 1994.
(28) Hagfeldt, A.; Bjorksten, U.; Gratzel, M. *J. Phys. Chem.* **1996**, *100*, 8046−8048.

(29) Dolata, M.; Kedzierzawski, P.; Augustynski, J. *Electrochim. Acta* **1996**, *41*, 1287−1293.
(30) Bard, A. J.; Faulkner, L. R. *Electrochemical Methods*; John Wiley & Sons: New York, 1980.
(31) Kavan, L.; Grätzel, M.; Gilbert, S. E.; Klemenz, C.; Scheel, H. J. *J. Am. Chem. Soc.* **1996**, *118*, 6716−6723.
(32) Tafalla, D.; Salvador, P. *J. Electroanal. Chem. Interfacial Electrochem.* **1989**, *270*, 285−295.
(33) Candal, R.; Zeltner, W. A.; Anderson, M. A. *J. Adv. Oxid. Technol.* **1998**, *3*, 270−276.
(34) Xu, Q.; Anderson, M. A. *J. Mater. Res.* **1991**, *6*, 1073−1081.
(35) Xu, Q.; Anderson, M. A. *J. Am. Ceram. Soc.* **1994**, *77*, 1939−1945.

same withdrawal speed. (v) Specimens were sintered at 300 °C for 5 h. This procedure yielded homogeneous and reproducible films of TiO$_2$. XRD analysis of the film (STOE-Darmstad, Nicolet Instrument Corp.) detected only the anatase form of TiO$_2$. Gravimetric estimation indicated that the films were approximately 85 nm thick.

**Optical (UV−Visible Spectroscopic) Measurements.** UV−visible measurements were made in situ in a quartz cell designed specifically for the experiment. Circular quartz disks (ESCO Products; 12.7 mm diameter) were coated once with an aqueous TiO$_2$ sol at the same withdrawal speed as used for the Ti plate. The disks were sintered at 300 °C for 5 h. A small quantity of thionine (5 mL, of 5 mM) was introduced into the cell and allowed to adsorb onto the TiO$_2$ surface for 4 h. The amount of strongly adsorbed thionine was measured after thoroughly rinsing the TiO$_2$-coated disk and immersing again in water. A monolayer of thionine was estimated to be $1 \times 10^{14}$ molecules/cm$^2$.

**Electrochemical and Photoelectrochemical Measurements.** Electrochemical and photoelectrochemical measurements were performed in a single-compartment rectangular Teflon cell of 30 mL capacity. The cell contained a circular window of borosilicate glass, 0.25 mm thick. A donut-shaped platinum counter electrode with a 4.6 cm$^2$ opening on the inside of the window allowed for illumination of the titania-coated working electrode. A circular opening 1 cm from and opposite to the counter electrode exposed 4.6 cm$^2$ of the working electrode to solution and UV irradiation, where indicated. The counter electrode was approximately of the same area. UV light passed through 1 cm of solution before reaching the surface of the electrode. A bridge tube with a Vycor frit was connected to a saturated calomel reference electrode (SCE) and placed 5 mm in front of the working electrode. All potentials were reported versus SCE. The bridge tube was 4 mm thick, blocking only a small fraction of the UV light during irradiation. No attempt was made to block room light during nonilluminated experiments, since photoactivation of TiO$_2$ only occurs upon radiation with wavelengths of ca. 385 nm or less.

Electrochemical impedance spectroscopy analysis and the electrochemical and photoelectrochemical measurements were performed with a Princeton Applied Research (PAR) model 6310 AC impedance system. The frequency response of the electrode was analyzed in the range 10−30 kHz. The data were analyzed quantitatively using the microcomputer program EQUIVCRT.[36] A 450 W Xe−Hg arc lamp (Oriel model 66024) was used as a UV light source. The light was passed through a water filter to remove IR radiation and a then through band-pass filter (230−450 nm, Oriel). The intensity of the light at the photoelectrode was 15.2 mW/cm$^2$, as measured with a photometer (International Light Inc., Model IL 1400A). The electrolytes were usually aqueous solutions of 0.01 M NaCl (other concentrations are indicated where appropriate). NaCl does not complex strongly with TiO$_2$ and was thus chosen as an inert supporting electrolyte. The salt also performed as an ionic strength buffer, diminishing the effect of the double-layer capacitance. Since the space charge and double-layer capacitances are in series, the smaller of the two will dominate. This method allowed for analyses of the space charge capacitance alone. Thus, the addition of small amounts of acid, base, or phosphate did not greatly affect the ionic strength. As an example, no significant difference existed between flat-band potentials
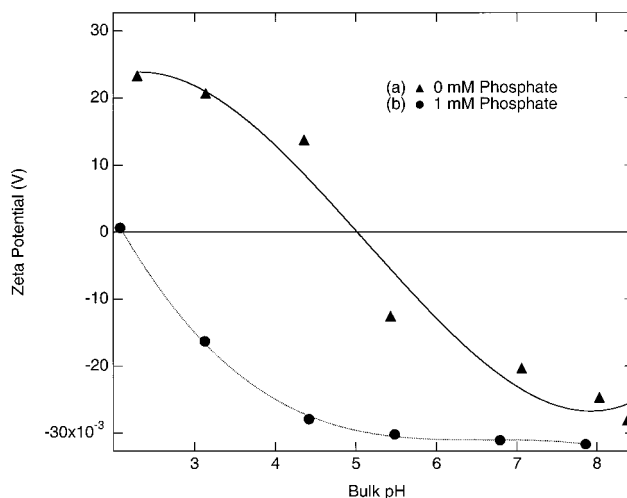
(36) Boukamp, B. A. *EQUIVCRT*; EG&G PARC: Enschede, The Netherlands, 1993.



**Figure 1.** Electrophoretic mobility curves in 10 mM NaCl for a fired and crushed TiO$_2$ xerogel without (a) and with (b) 1 mM phosphate. Despite the fact that phosphate is not classified as a potential-determining ion, the pzzp shifts by 3 pH units. Phosphate is known instead as a specifically adsorbed ion.

determined in 10 mM NaCl and those determined in test solutions of 100 mM NaCl. When phosphate was required, KH$_2$PO$_4$ (Aldrich) was added to the solutions. The pH's of the solutions were adjusted with 0.1 M HCl or KOH aqueous solutions, under nitrogen atmosphere, to prevent the introduction of CO$_2$. Where phosphate was concerned, the pH ranges used were restricted such that H$_2$PO$_4^-$ would be the dominant phosphate species in solution. NaCl solutions were bubbled with nitrogen for 30 min prior to the adjustment of their pH's. Most experiments were conducted under N$_2$ atmosphere (other atmospheres are specified where appropriate).

**Electrophoretic Mobility Measurements.** The electrophoretic mobility of TiO$_2$ particles in 0.010 M NaCl was measured with a PenKem System 3000 microelectrophoresis analyzer with and without 0.001 M KH$_2$PO$_4$. A 5 mL portion of aqueous TiO$_2$ sol was dried and fired at 300 °C for 5 h to make an unsupported TiO$_2$ membrane. TiO$_2$ suspensions were prepared by grinding the TiO$_2$ membrane in an agate mortar in the presence of the electrolyte. The final concentration of TiO$_2$ in each suspension was 0.2 g/L. The pH's were adjusted by adding appropriate amounts of 0.1 M HCl or KOH, under N$_2$ atmosphere. The samples were stored under N$_2$ atmosphere for 12 h at room temperature after pH adjustment in order to allow the surfaces to equilibrate with the solutions. The pH's were measured again before measuring the mobilities and readjusted as necessary.

## Results and Discussion

The charge on the surface of an oxide can be determined by factors such as pH, the presence or absence of other potential-determining ions, or even trapped species that exist as surface states. Electrophoretic mobility is the most common technique for investigating changes in surface charge.[17] With this technique, the migration of suspended particles is quantified under an electric field. Figure 1a shows the results of electrophoretic mobility measurements of a ground TiO$_2$ xerogel suspension. The isoelectric pH is close to 5. A high isoelectric pH is associated with a less acidic surface, i.e., a high affinity for protons and a more positively charged surface. With the addition of phosphate (Figure 1b), the isoelectric pH of the TiO$_2$ surface shifts by 3 pH units to pH 2. With this adsorption, the surface becomes significantly more negative for a given
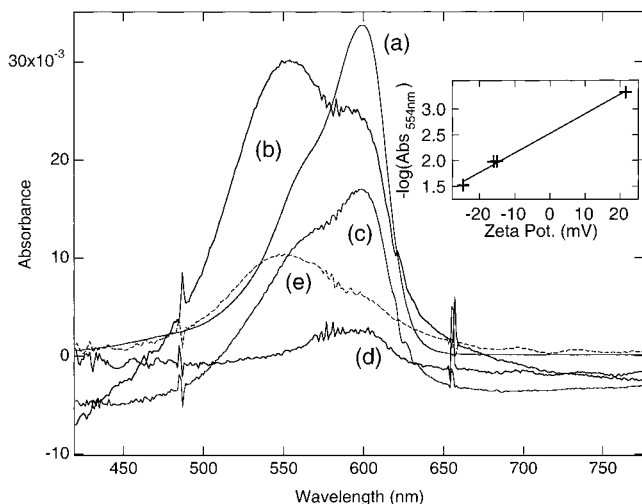
**Figure 2.** UV−visible absorption spectra of the remaining thionine adsorbed onto TiO₂ after thorough rinsing. Adsorption experiments were conducted at various pH values and demonstrate that thionine adsorption is dependent on the $\zeta$ potential in a quantifiable way. The bulk absorption spectrum of a micromolar solution of thionine in water is shown in (a). Spectra of thionine adsorbed onto TiO₂ at pH 8 (b), pH 6 (c), pH 3 (d), and pH 3 in the presence of phosphate (e) show that adsorption is dependent upon the charge of the oxide surface. The inset shows the dependence of the absorption peak at 554 nm on $\zeta$ potential. Note the similarity between the absorptions with and without phosphate at the same $\zeta$ potential.

pH. The effects of specifically adsorbed ions on oxide surface charges have been well documented.[17,20,37] Phosphate is known to adsorb strongly to TiO₂[26,38] over a wide pH range,[22] and its adsorption is independent of applied potential.[39]

The effect of changes in surface charge was also monitored with a cationic probe molecule easily detected by UV−visible (UV−vis) spectroscopy. Thionine, a cation with a strong visible absorption band at 600 nm and a shoulder at 566 nm, was chosen for this purpose. Thionine and several related compounds were previously investigated as dye sensitizers for use with semiconductor oxides.[40−42] Shown in Figure 2a is the spectrum of bulk thionine in aqueous solution. Other researchers have shown that thionine adsorbs onto an SnO₂ suspension through an electrostatic interaction, resulting in a blue shift of the thionine absorption peak at 600 nm.[40] The shift in the absorption spectrum has been attributed to the aggregation of thionine molecules near the charged surface. Our results show that this interaction is also present for nanocrystalline TiO₂ coatings in water and that it is robust and highly pH dependent. A TiO₂-coated quartz disk was thoroughly rinsed with water after exposure to thionine solution for 4 h at various pH values. The coated disk was then examined with UV-vis spectroscopy. In Figures 2b−e are shown the spectra of thionine bound to a TiO₂ film after exposure to thionine-containing solutions. At pH 8 (Figure 2b), where the oxide surface is most negatively charged, cationic thionine binds most strongly to the TiO₂ surface. Also note that, with this

adsorption, the UV−vis absorption maximum of thionine shifts to 554 nm, a significant blue shift. This, combined with the fact that rinsing cannot remove the thionine, indicates the bond between the thionine and TiO₂ is robust. The shift is most pronounced at high pH, as seen in Figure 2b, which shows the highest absorption at 554 nm of all three pH values. Figure 2c, at pH 6, shows an intermediate amount of absorption at 554 nm, but significant absorption is also seen at 600 nm. The slightly negative TiO₂ surface appears to be retaining a mixture of less concentrated thionine and more strongly bound, or aggregated, thionine (554 nm) at this pH. Figure 2d shows the results at pH 3, where only a small amount of loosely bound thionine is evident and no evidence of strongly bound thionine is seen. The TiO₂ surface was also modified by the presence of phosphate in solution at pH 3. As seen in Figure 1, the addition of phosphate to the system results in a more negative TiO₂ surface at a given pH. With phosphate present during adsorption at pH 3, the strong adsorption of thionine increases significantly. This is shown in Figure 2e. The additional absorption signal at 554 nm is now equivalent to that seen at pH 6. The presence of phosphate sufficiently modifies the surface charge to force thionine binding to a formerly positive TiO₂ surface, equivalent to changing the surface charge by 3 pH units. This demonstrates the ability to tune the adsorption of charged molecules at a given pH by controlling surface charge with the adsorption of specifically adsorbed ions such as phosphate. This provides a new tool for controlling the adsorption of dye molecules. Quantification of thionine adsorption was also used to show that the TiO₂ film resulted in an approximately 35-fold enhancement of surface area, if monolayer coverage was assumed.

Plotting photocurrent/potential curves is a common technique for investigating electrochemical behavior of nanocrystalline electrodes, including that of the flat-band potential. Porous nanocrystalline oxides present a particular challenge because of the high density of surface states, nonuniform surfaces, and recombination centers on these surfaces. Analysis of these data can yield information about processes at the surface. For example, changes in the flat-band potential of oxide surfaces such as TiO₂ are governed by the concentration of the potential-determining ions H⁺ and OH⁻ and such changes can be predicted by the Nernst equation.[43,44] Irradiation of the surface with light of energy greater than that of the band gap causes the formation of electron hole pairs; a potential bias higher than that of the flat-band potential produces a bending of the conductive band and causes these holes to separate and photocurrent to flow.[30] The potential at which photocurrent begins to flow can be used to estimate the flat-band potential of a semiconductor. While considerable doubt exists as to whether band bending actually occurs in nanocrystalline domains, studies have shown that a potential bias positive of the flat-band potential can increase photocatalytic efficiency in these nanocrystalline membranes.[27] Our experiments using the onset-potential method showed a Nernstian response to changes in pH for a wide range of pH values. Figure 3 (inset) shows the onset potential changes with pH for the whole range of pH 2−12. The overall slope calculated for these measurements was −56 mV/pH unit, consistent with many previous studies conducted on similar surfaces. These data indicate that hydronium/hydroxide adsorption processes continue for a wider pH range (2−12) than the electrophoretic mobility experiments would suggest.

(37) Tejedor-Tejedor, M. I.; Anderson, M. A. *Langmuir* **1990**, *6*, 602−611.

(38) Flaig-Baumann, R.; Hermann, M.; Boehm, H. *Z. Anorg. Allg. Chem.* **1970**, *372*, 296.

(39) Kazarinov, V. E.; Andreev, V. N.; Mayorov, A. P. *J. Electroanal. Chem. Interfacial Electrochem.* **1981**, *130*, 277−285.

(40) Liu, D.; Kamat, P. V. *Langmuir* **1996**, *12*, 2190−2195.

(41) Patrick, B.; Kamat, P. V. *J. Phys. Chem.* **1992**, *96*, 1423−1428.

(42) de Tacconi, N. R.; Carmona, J.; Rajeshwar, K. *J. Electrochem. Soc.* **1997**, *144*, 2486−2490.

(43) Tomkiewicz, M. *J. Electrochem. Soc.* **1979**, *126*, 1505−1510.

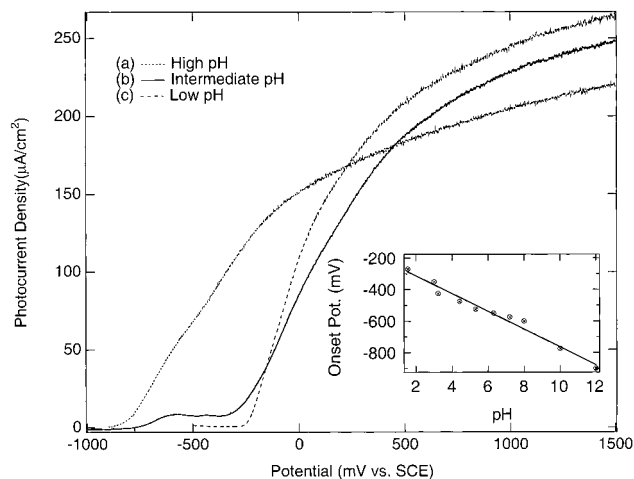(44) Lantz, J. M.; Baba, R.; Corn, R. M. *J. Phys. Chem.* **1993**, *97*, 7392−7395.

**Figure 3.** Photocurrent/potential curves used to determine flat-band potentials showing that the onset potential is dependent on the concentration of potential-determining ions. Characteristic behaviors are shown at high pH (12.1) in (a), at intermediate pH (6.0) in (b), and at low pH (1.55) in (c). The plateau that precedes the onset of significant current at intermediate pH has been associated with slow electron transport to the backcontact. The addition of phosphate had no effect on the plateau, the photocurrent/potential curve, or $V_{on}$. The inset shows the pH dependence of flat-band potentials calculated by the onset-potential method.

At intermediate pH values, small deviations from the linear fit of onset potential versus pH were observed (Figure 3 (inset)). At these same pH values, changes in the shape of the photocurrent/potential graph made precise determination of the flat-band potential more difficult. This slow rise and plateau of current are pH dependent and are shown for three pH values in Figure 3. Low- and high-pH onset-potential measurements each show a single, sharp onset of photocurrent, and the determination of the flat-band potential is quite simple. At intermediate pH, however, a "plateau" is observed. Previous papers have associated this plateau with the slow transport of excess electrons from the backcontact to the bulk of the electrode.[23,45] For intermediate pH values, the onset potential of this plateau provided an adequate determination of the flat-band potential, as seen in the inset of Figure 3. We observed no effect on the shape or onset potential of the plateau or of any other aspect of the photocurrent/potential curve with the addition of phosphate, suggesting the presence of this ion does not affect electron transport to the backcontact under UV irradiation. These results are consistent with those of most studies of adsorption of inorganic ligands and their effect on the onset potential.[46]

The ac response of the Ti/nanocrystalline $TiO_2$ system was examined with impedance spectroscopy and analyzed with the use of equivalent circuits. Nyquist plots of these data reflect specific characteristics of the system. This is demonstrated in Figure 4, which shows plots of data (as open symbols) and resulting fits of equivalent circuits (as dots) for several different systems at pH 4.45 and −100 mV bias for the frequency range 0.01−30 kHz. Figure 4a shows the Nyquist plot of the impedance response for a $TiO_2$ electrode in a dilute NaCl solution. The equivalent circuit in Figure 4a (inset) was used to model this behavior. The high-frequency semicircular arc is believed to be due to electron transfer in the porous $TiO_2$ coating. Without

(45) Konenkamp, R.; Henninger, R.; Hoyer, P. *J. Phys. Chem. B.* **1993**, *97*, 7328−7330.
(46) Finklea, H. O. *Semiconductor Electrodes; Finklea, H. O., Ed.; Elsevier: 1988; p 74.*
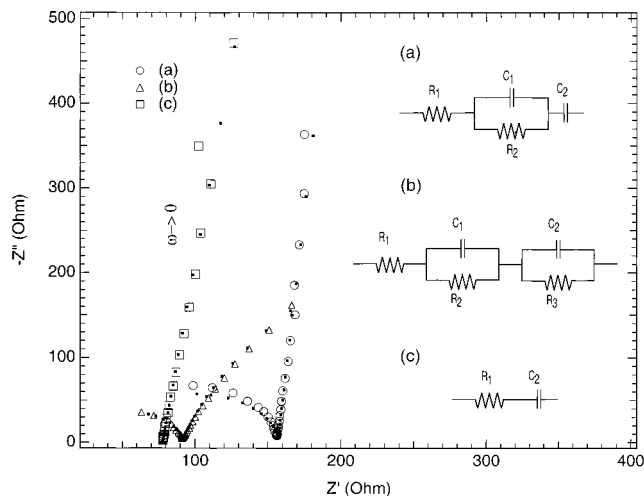


**Figure 4.** Examples of Nyquist plots and equivalent circuits used to model impedance spectroscopy data for the determination of flat-band potentials: (a) (○) $TiO_2$-coated porous electrode; (b) (△) $TiO_2$-coated porous electrode under UV irradiation; (c) (□) uncoated, sintered-titanium backcontact (with a thin oxide coating produced by thermal oxidation during sintering). Dots show results of equivalent circuit fits. These data were taken at pH 4.45 with a −100 mV bias in 10 mM NaCl. Electrode area: 4.6 cm². Actual Boukamp models used a constant phase element (CPE) where capacitors are shown. Parameters used for the CPE suggest behavior similar to that of a capacitor. Values of $C_2$ were used for the Mott−Schottky determination of the flat-band potentials.

the porous oxide coating, this arc is all but eliminated, as shown by impedance measurements made on sintered-titanium backcontacts alone (Figure 4c). Only a nearly unnoticeable arc in this frequency range remains. This small arc is believed to be due to processes on the thin oxide coating on the titanium backcontact, produced during the sintering process. If this small arc is ignored, this system can be truncated with the simplified equivalent circuit in Figure 4c (inset). At lower frequencies, a straight line is indicative of capacitive behavior. This is modeled with the parameter $C_2$ in Figure 4a (inset).

UV irradiation of the electrochemical cell during impedance analysis (Figure 4b) decreased the radius of the high-frequency semicircular arc, demonstrating the increased conductivity of the $TiO_2$-coated porous film. This is reflected in the equivalent-circuit model (Figure 4b (inset)), where the value of resistor $R_2$ decreases with UV irradiation (not shown). UV irradiation also changed the low-frequency straight-line capacitive behavior shown in Figure 4a,c into a semicircular arc, indicative of a redox reaction, likely the photooxidation of water. This is modeled in Figure 4b (inset) with the addition of the resistor $R_3$. The semicircle radius decreased with the application of more positive potentials, indicating that electrical enhancement of the photooxidation process reduces the charge-transfer resistance associated with the oxidation. Interestingly, this enhancement effect was more notable in uncoated than in coated electrodes; uncoated electrodes, with little or no nanocrystalline structure, showed a more substantial reduction in charge-transfer resistance for a given applied potential (data not shown). This is not surprising. Since the width of the semiconductor depletion layer is too large to be contained in the nanocrystalline colloidal particles that make up the coating, it is expected that facilitation of the depletion layer formation by applied potential would be difficult here. In fact, other authors have shown that applied potential is expected to have a less significant effect on
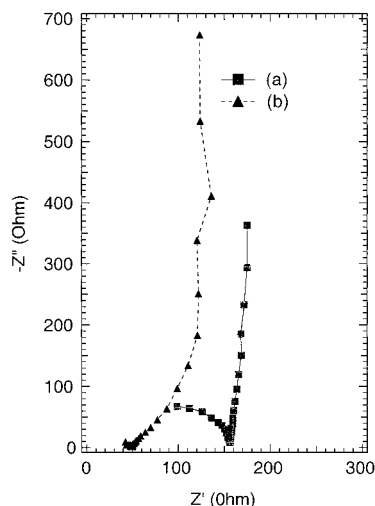
**Figure 5.** Nyquist plots of impedance data for an electrode in (a) 10 mM NaCl and (b) 10 mM NaCl and 1 mM KH₂PO₄. The addition of phosphate to the solution eliminates the high-frequency semicircular arc, indicating the reduced resistance of the TiO₂ film. Note also the increase in the imaginary impedance.

the efficiency of photogenerated electron–hole separation in nanocrystalline systems compared to that in compact electrodes.[24,28,47] In other words, as more nanocrystalline material coats the surface, photooxidation occurs farther away from the backcontact (where potential bias has an effect) and rates of photocatalysis improvement with applied potential decrease. Authors agree that charge-transfer processes in nanocrystalline systems are governed more by surface charge-transfer rates than by applied potentials.[48–50]

The introduction of phosphate to the system also strongly affected the impedance results. Figure 5 shows a Nyquist plot of impedance results from an electrode (a) with and (b) without phosphate in solution. Note the high-frequency arc has all but disappeared, indicating that phosphate reduces the electron-transfer resistance in the porous TiO₂ coating. A similar effect is seen in Nyquist plots at lower pH, where the radius of the high-frequency semicircular arc decreases from typical values of $R_2$ from near 80 Ω at pH 4.45 to less than 10 Ω at pH 3.2. These results suggest that surface acidity, not just phosphate adsorption, plays a role in the conductivity of the TiO₂ film. The addition of phosphate increases and slightly distorts the imaginary component of the impedance seen at low frequencies. An increase in proton conductivity for TiO₂ xerogels in air has also been reported as a consequence of changes in surface acidity, including phosphate adsorption.[15]

Equivalent circuits developed to model the impedance results were used for Mott–Schottky analysis. Values for each element in the equivalent circuit were calculated at each pH and applied potential from the impedance data, and the space charge capacitance was estimated from element $C_2$, calculated from a constant-phase element (CPE). Porous materials can produce behavior consistent with a CPE,[51] and when the calculated CPE exponential

is close to unity, the behavior closely matches that of a capacitor,[36,52] as was the case for our system. Results from Mott–Schottky analysis of the impedance response obeyed the Mott–Schottky relation for a wide pH range and were used to estimate flat-band potentials. Capacitance values for Mott–Schottky analysis were taken from $C_2$ in the equivalent circuit and used to determine the flat-band potentials of the system at various pH values using Mott–Schottky plots (not shown). Mott–Schottky analysis consists of a plot of $1/C_2{}^2$ versus potential. Materials that show Mott–Schottky behavior show a linear relationship between $1/C_2{}^2$ and potential; the $x$ intercepts of such plots are estimations of the flat-band potentials. These values come from the capacitive, low-frequency behaviors that form straight lines on Nyquist plots, notable in Figure 4a,c. Calculated capacitance values at potentials well below the flat-band potentials were found to be approximately 35 $\mu F/cm^2$, in reasonable agreement with previously published values of space charge capacitances for nanocrystalline Ti/TiO₂ electrodes.[53] Capacitance values for the TiO₂-coated porous electrodes were only slightly higher than values calculated for the uncoated, sintered backcontact, indicating values for $C_2$ only probed the oxide coating on the titanium backcontact and a fraction of the porous coating. If the results represented the whole coating, one would expect that $C_{sc}$ should scale with the additional surface area gained with the nanoporous coating (similar to the 35-fold increase in thionine adsorption observed with the addition of the porous coating discussed earlier). This corresponds with results from other studies of nanocrystalline TiO₂ that suggest that the TiO₂ backcontact dominates the ac impedance response in this frequency range.[28] Thus, the oxide coating on the backcontact likely dominates the measured flat-band potential. The fact that the oxide coating on the back-contact also governs the impedance response in this frequency range helps to explain the capacitor-like response of the rough electrode. Mott–Schottky estimated flat-band potentials matched results from the onset-potential experiment for a limited pH range only. This is shown in Figure 6, which shows Mott–Schottky estimated flat-band potentials (part a) and a fit of onset potential results (part c) for comparison. For the pH range 3–7, approximately Nernstian behavior (−59 mV/pH slope) was evident for the Mott–Schottky results, with values corresponding closely to onset-potential measurements. Above pH 7, the calculated flat-band potential was insensitive to pH changes, contrary to onset-potential results, which tracked closely with pH in a Nernstian fashion for the entire pH range 2–12. Other authors have also reported insensitivity of flat-band potentials at high pH.[53] The flattening of the Mott–Schottky determined flat-band potential data show a similarity to the electrophoretic mobility results, which also track with pH in the same pH range. The similarity between these results may suggest that both techniques measure changes at or near the shear plane, the location of which is not clearly defined,[17] and for both cases, the potential at the shear plane is fixed by a saturation of specifically adsorbed negative charges above pH 7.

For the equivalent circuits calculated in the presence of phosphate, values of the CPE exponent were roughly 10% lower than those calculated without phosphate at the same pH. Nyquist plots of impedance data taken in

(47) Poznyak, S. K.; Kokorin, A. I.; Kulak, A. I. *J. Electroanal. Chem. Interfacial Electrochem.* **1998**, *442*, 99–105.

(48) Vinodgopal, K.; Hotchandani, S.; Kamat, P. V. *J. Phys. Chem.* **1993**, *97*, 9040–9044.

(49) Hodes, G.; Howell, I. D. S.; Peter, L. M. *J. Electrochem. Soc.* **1992**, 139.

(50) O'Regan, B.; Moser, J.; Anderson, M. A.; Gratzel, M. *J. Phys. Chem.* **1990**, *94*, 8720–8726.

(51) Wang, J. C.; Bates, J. B. *Solid State Ionics* **1986**, *18/19*, 224.

(52) Jiang, S. P.; Love, J. G.; Badwel, S. P. S. *Electrical Properties of Oxide Materials*; Trans Tech Publications: Aedermannsdorf, Switzerland, 1997; Vols. 125–126, pp 81–132.

(53) Nogami, G.; Ogawa, Y.; Ogawa, Y. *J. Electrochem. Soc.* **1988**, *135*, 3008–3015.
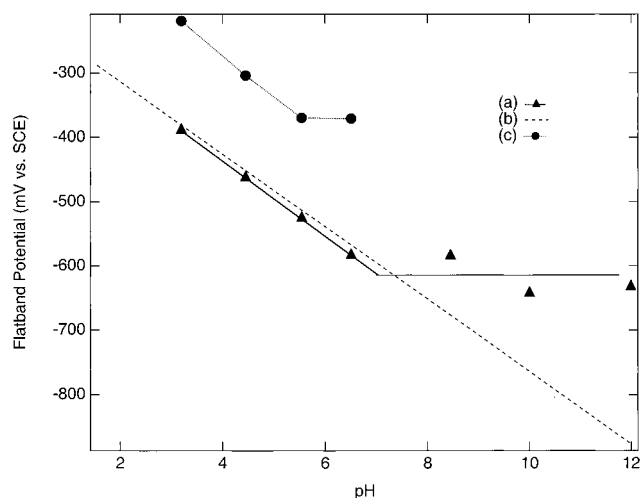
**Figure 6.** (a) Flat-band potentials of a coated porous TiO₂ electrode, determined by Mott−Schottky analysis, as a function of the bulk solution pH in 10 mM NaCl. (b) Fit of onset potentials from Figure 3 (inset) shown for comparison. (c) Potentials of the capacitance peak in 1 mM $KH_2PO_4$ and 10 mM NaCl as a function of pH.
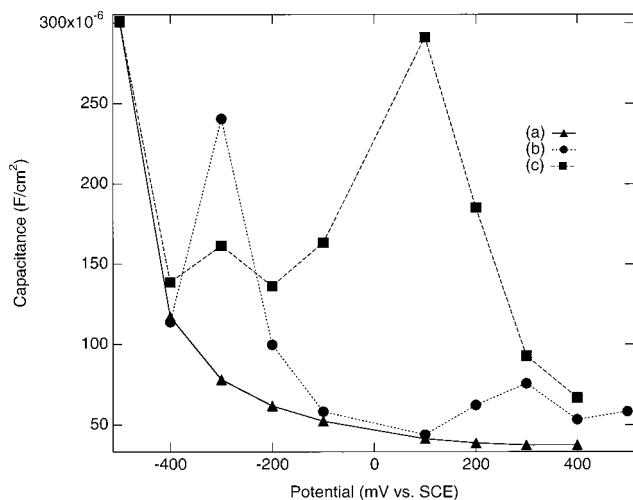


**Figure 7.** Plots of capacitance per unit geometric area ($C_2$/cm²) as a function of potential for (a) 1 mM NaCl, (b) 1 mM NaCl and 1 mM phosphate, and (c) 1 mM NaCl under UV irradiation. The additional charge on the surface due to the phosphate adsorption results in a capacitance peak at a particular potential. The potential at which this peak occurs is dependent upon the pH. The appearance of the peak is similar to that created by UV irradiation.

the presence of phosphate (Figure 5) reflected this, with a deviation from the largely straight-line capacitive behavior seen without phosphate at low frequencies. The key difference with the addition of phosphate is noted in Figure 7, which shows the change in the value of the capacitance, $C_2$, used in the equivalent circuit for the determination of the flat-band potential at pH 4.45. As expected for a system showing Mott−Schottky behavior, as the applied potential approaches the flat-band potential, the capacitance increases dramatically, indicating band flattening. With the addition of phosphate, a capacitance "spike" is notable near −300 mV (Figure 7b). Similar behavior was observed when samples were analyzed at other pH values, and the potential at which this occurred tracked in a nearly Nernstian fashion (−64 mV/pH unit)

for a limited pH range. This is shown in Figure 6b. The additional capacitance occurs at 150 mV above the flat-band potential, or about 3 pH units for a Nernstian system. This is similar to the change seen in the pH of zero charge as measured by the electrophoretic mobility. To confirm that this effect is due to adsorbed phosphate and not to ionic strength or other solution effects, TiO₂ electrodes were also exposed to phosphate solutions and rinsed, and impedance spectroscopy was conducted on electrodes in NaCl alone. Similar results were also seen in this experiment.

Results from electrophoretic mobility experiments were used to help understand the additional capacitance at potentials positive of the flat-band potential. Electrophoretic mobility can be used to examine surface acidity. Adsorption from a 1 mM phosphate solution onto TiO₂ adds an additional negative surface charge at low pH equivalent to making the TiO₂ surface less able to hold protons (more acidic) by 3 pH units. Recently published results from our laboratory demonstrated that the adsorption of phosphate onto a mesoporous TiO₂ membrane can increase the proton conductivity. In a Nernstian system, a change of 3 pH units should correspond to an approximately 180 mV change in the flat-band potential. In our system, the adsorption of phosphate was shown to make the surface 3 pH units more acidic, by electrophoretic mobility measurements, and to add an additional capacitance 150 mV positive of the flat-band potential, by analysis of impedance spectroscopy data. Our laboratory recently reported a correlation between the proton conductivities of several oxide materials and their isoelectric pH values as determined by electrophoretic mobility measurements.[16] It has also been shown that the addition of phosphate and changes in pH improve proton conductivity on TiO₂.[15]

Investigation of a similar system supports the conclusion that these changes are related. Irradiation of TiO₂ in the absence of oxygen and other easily reducible species has been reported to cause a buildup of negative charge on the surface. This has been shown by Dunn et al. with measurements of the electrophoretic mobility of a TiO₂ suspension under UV irradiation.[54] These authors found that the UV irradiation results in a negative shift (0.5 pH unit) in the isoelectric point of the TiO₂. The direction of the shift is the same as that due to phosphate adsorption. Similarly, Figure 6c shows the change in capacitance as measured by fits of impedance data in $C_2$ of the equivalent circuit. A capacitance spike positive of the flat-band potential is seen for both the phosphate and the UV-illuminated Ti/TiO₂ systems. Mott−Schottky analysis of these data suggests a 500 mV shift in the flat-band potential of the illuminated system compared to the unilluminated system. Hagfeldt et al. also reported that Mott−Schottky derived flat-band potentials for the Ti/TiO₂ system shift by 500 mV with UV irradiation.[28] Although the reported shift in electrophoretic mobility with UV irradiation is small compared to the change in the flat-band potential, we believe that irradiation of the TiO₂ surface also activates more of the TiO₂ electrode. Data taken on uncoated, sintered-Ti backcontacts show only a small shift in flat-band potential upon irradiation. Hagfeldt et al. also reported similar results for sintered backcontacts.

UV irradiation increases the conductivity of the TiO₂ surface and creates a capacitance "spike", similar to that seen with phosphate adsorption. We also believe the

(54) Dunn, W. W.; Aikawa, Y.; Bard, A. J. *J. Am. Chem. Soc.* **1981**, *103*, 3456−3459.

change in the capacitance due to phosphate adsorption is likely related to increased conductivity of the $TiO_2$ coating. However, since no change is seen in the initial "plateau" of photocurrent potential curves (believed to be associated with the electron transport to the backcontact) with phosphate adsorption, the effect of phosphate may not be as important under UV irradiation. Taffalla et al.[32] have reported that changes in the local pH brought about by irradiation affected the flat-band potential. Shifts in the electrophoretic mobility suggest changes in the local pH at the surface of the oxide. However, if the local solution pH is calculated using the Boltzmann correction according to the method of Tejedor-Tejedor et al.,[37] the change in pH is not consistent with the direction of the shift in flat-band potential.

## Conclusion

Control of $TiO_2$ surface properties was accomplished by altering the pH of the solution, by the adsorption of specifically adsorbed ions such as phosphate, or by a combination of both. We have shown that the surface adsorption of charged species can be controlled by tuning the surface $\zeta$ potential with a specifically adsorbed ion such as phosphate or with changes in the pH. Impedance spectroscopy shows that that the measured flat-band potential of these electrodes has a Nernstian response with pH and that adsorption of phosphate changes the space charge capacitance of these nanocrystalline electrodes. This change is believed to be associated with an increase in the conductivity of the electrode with phosphate adsorption as demonstrated in Nyquist plots. These findings are now proving useful for the development of a new type of $TiO_2$-based thin-film fuel cells and may help to improve both the photocatalytic degradation of organic contaminants and the functionalization of these oxide surfaces.